TOMASZ JANOSZEK[1*]

# THE ASSESSMENT OF LONGWALL WORKING STABILITY BASED ON THE MOHR-COULOMB STRESS CRITERION – NUMERICAL ANALYSIS

The use of computer techniques at the design stage of industrial facilities is essential in modern times. The ability to shorten the time required to develop a project and assess the safety of the use of assumptions, often enables the reduction of the costs incurred in the future. The possibility to skip expensive prototype tests by using 3D prototyping is why it is currently the prevailing model in the design of industrial facilities, including in the mining industry. In the case of a longwall working, its stability requires the maintenance of the geometric continuity of floor rocks in cooperation with a powered roof support.

The paper investigates the problem of longwall working stability under the influence of roof properties, coal properties, shield loading and the roof-floor interaction. The longwall working stability is represented by an index, factor of safety (FOS), and is correlated with a previously proposed roof capacity index 'g'. The topic of the paper does address an issue of potential interest.

The assessment of the stability of the roof in longwalls was based on the numerical analysis of the factor of safety (FOS), using the Mohr-Coulomb stress criterion. The Mohr-Coulomb stress criterion enables the prediction of the occurrence of failures when the connection of the maximum tensile principal stress $\sigma_1$ and the minimum compressive principal stress $\sigma_3$ exceed relevant stress limits. The criterion is used for materials which indicates distinct tensile and compressive characteristics. The numerical method presented in the paper can be utilized in evaluating the mining natural hazards through predicting the parameters, which determine the roof maintenance in the longwall working.

One of the purposes of the numerical analysis was to draw attention to the possibilities that are currently created by specialized software as an important element accompanying the modern design process, which forms part of intelligent underground mining 4.0.

**Keywords:** longwall mining, stability, powered support, numerical analysis, roof fall

1    CENTRAL MINING INSTITUTE, 1 GWARKÓW SQ., 40-166 KATOWICE, POLAND

*    Corresponding author: tjanoszek@gig.eu
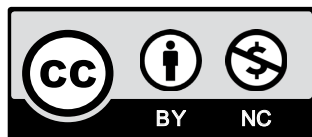
# 1. Introduction

The stability of longwalls mainly depends on the geological and mining conditions as well as properly selected shields for mining conditions. The loss of stability in longwalls presents a risk for the mining crews extracting coal, due to roof falls hazard. The roof fall hazard is a prominent hazards in underground hard coal mines. The loss of longwall stability, which reveals itself in the form of minor or major roof falls (Fig. 1), generally exists in all underground mines and has been confirmed in the form of statistical data from hard coal mines located in Poland, as well as in the USA, India, Iran, Turkey and China (Biliński, 1968; Ghasemi et al., 2017; Gu et al., 2018; Iannacchione et al., 2007; Mark et al., 2011; Martyka et al., 2013; Palei et al, 2008).

Based on research aimed at analyzing the phenomena that influence roof fall hazards in caving longwalls in the Central Mining Institute's (CMI) as well as in-situ observations of several underground situations in longwalls, mainly located in Poland, it was concluded that there is a strong relationships between the method for selecting shields on the roof stability in a longwall. An incorrectly selected shield may result in a situation where the shield support does not sufficiently interact with the rock mass. The proper interaction of shield support with the rock mass is one of the most important parameters which determines the condition in which the longwall working satisfies its functions in the production process and ensures work safety for miners (Rajwa et al., 2020; Walentek et al., 2009).

The major symptoms of the loss of the stability in the working of a longwall are roof falls (Fig. 1), whereby pieces of material (Fig. 1-1) detach from the roof ahead of the canopy tip (Fig. 1-2) and fall onto the armored face conveyor (Fig. 1-3). These may lead to some form of breakage, but generally the face itself will not be delayed to any significant degree unless it is an on-going problem (Rajwa et al., 2020; Rajwa et al., 2019).
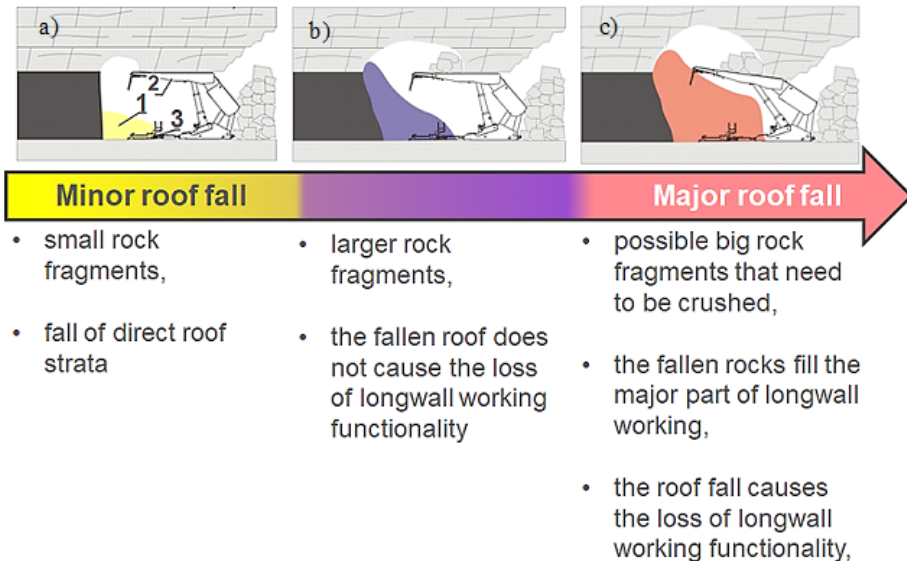


Fig. 1. Scheme of a roof fall in a longwall working: a – minor roof fall, b – medium roof fall, c – major roof fall, 1 – roof fall, 2 – canopy (powered support), 3 – armored face conveyor (AFC)

The method for the assessment of the stability of longwalls in underground hard coal mines, which are mainly in Poland, is based on the calculations of the roof bearing capacity called index 'g' (Prusek et al., 2017). Index 'g' is a result of research and observations undertaken in the CMI and which were aimed at analyzing the phenomena that influence roof fall hazards in caving longwall. The result of this research is an empirical method for selecting shields for mining conditions based on the calculations of the roof bearing capacity, developed by author (Biliński, 1968). The index 'g' is calculated with Equation (1) (Biliński, 1968; Prusek at al., 2017).

$$Roof\ bearing\ capacity\,(g) = \frac{1}{0.006 + \dfrac{\dfrac{0.05}{UCS}}{0.012 \cdot \dfrac{Mp}{Mq} + 0.02} + 0.3} \tag{1}$$

where uniaxial compressive strength (UCS) is a parameter determined based on tests in a given longwall, as well as values of support capacity moment ($M_p$ in unit [MNm]) and rock mass load moment ($M_Q$ in unit [MNm]).

The value of index 'g' which describes the stability of the roof in a longwall is based on the assumed criteria as shown in Table 1 (Prusek at al., 2017).

TABLE 1

Value of index 'g' which describes roof maintenance in the longwall working (Prusek at al., 2017)

| Value of index 'g' | Roof maintenance in the longwall working |
|---|---|
| $g < 0.7$ | Very bad roof maintenance |
| $0.7 \leq g < 0.8$ | Difficult conditions for roof maintenance |
| $g \geq 0.8$ | Good or very good roof maintenance |

A method based on the value of roof capacity index 'g' is currently one of the main methods applied in Polish underground mining in order to determine the conditions of roof maintenance in a longwall panel.

Another concept for assessing the risk of roof falls in the underground mining is presented in (Iannacchione et al., 2007). The authors present a method for determining risk of roof falls using a qualitative risk-analysis method, called the roof fall risk index (RFRI). Based on the statistical data analysis of values for the 226 measurement areas in underground coal mines in the USA, Iannacchione A. et al. (Iannacchione et al., 2007) developed a method for assessing the roof fall probability based on the RFRI values and divided into five categories: very unlikely (RFRI < 0.21), unlikely (0.21 < RFRI < 0.30), possible (0.31 < RFRI < 0.40), likely (0.41 < RFRI < 0.50) and very likely (RFRI > 0.50). Ghasemi et al. (Ghasemi et al., 2012) proposed a systematic methodology for assessing the roof fall risk during retreat mining based on the classic risk assessment approach. The proposed classification of roof fall hazard during retreat mining in the form of the level of roof fall risk ($R_{rf}$), when $R_{rf} < 28$ the roof fall risk category is low and at an acceptable level, but when $R_{rf} > 70$ the roof fall risk is unacceptable due to all parameters being in their most risky condition. Another methodology is presented in (Ghasemi et al., 2017) to assess the roof fall risk (RFS) using the fuzzy approach in order to identify the susceptibility of roof fall occurrence. In Table 2 was shown the making decision model components formed by (Ghasemi et al., 2017). The factors and sub-factors are the input data in RFS method.

The decision (AHP) model (Ghasemi et al., 2017)

| | Factors | | |
|---|---|---|---|
| | **Geological factors** | **Design factors** | **Operational factors** |
| 1. | Depth of cover | Panel width | Panel age |
| 2. | Roof rock quality | Panel uniformity | Supplemental support |
| 3. | Floor rock quality | Entry width | Cut sequence |
| 4. | Groundwater | Pillar design | Final stump |
| 5. | Overlying massive strata | Roof bolting | |
| 6. | Multiple-seam interaction | | |

The results indicate that this methodology is effective and efficient for assessing RFS. Duzgun and Einstein (Duzgun et al., 2004) proposed a method of roof falls risk based on an objective method to assess roof fall probability. This method which depends on the probability (P) of having a roof fall in order to appropriate actions can be taken and the success of such actions can be evaluated by using the decision analysis.

This article presents a method for the assessment of the stability of the roof in longwalls based on the calculations of the factor of safety (FOS). The index FOS is based on the Mohr-Coulomb stress criterion which enables the prediction of the occurrence of failure when the combination of the maximum tensile principal stress $\sigma_1$ and the minimum compressive principal stress $\sigma_3$ exceed their respective stress limits. The proposed method was developed in the SolidWorks Simulation module using the finite element method (FEM). The proposed method enabled investigators to determine the conditions for roof maintenance in a longwall, as well as to select proper shields for mining conditions.

The results obtained from the simulation were compared with the value of index 'g', which was calculated for the mining condition adopted in numerical modelling. The SolidWorks software was adopted for conducting finite element analysis (FEA) (Petrova, 2013).

## 2. The FOS assumptions

The Mohr-Coulomb stress criterion was used in order to define the safety factor called FOS index. This theory is based on the linear relationship between maximum tensile principal stress $\sigma_1$ and minimum compressive principal stress $\sigma_3$ (Labuz et al., 2012; Petrova, 2013). The FOS method assumes that, when their respective stress limits exceeds, the theory predicts the occurrence of failure in the following cases (Steffen, 2017):
   – In the case where ($\sigma_1 > 0$ and $\sigma_3 > 0$) all principal stresses in tension (positive) ($\sigma_1 \geq \sigma_{TL}$),
   – In the case where ($\sigma_1 < 0$ and $\sigma_3 < 0$) all principal stresses in compression (negative) ($|\sigma_3| \geq \sigma_{CL}$),
   – In the case where ($\sigma_1 > 0$ and $\sigma_3 < 0$) maximum tensile principal stress $\sigma_1$ in tension, but minimum compressive principal stress $\sigma_3$ in compression ($\sigma_1/\sigma_{TL} + |\sigma_3|/\sigma_{CL} \geq 1$).

The sub-index $\sigma_{TL}$ describes the tension tensile limit, while the sub-index $\sigma_{CL}$ describes tension compressive limit.

To summarise, the Mohr – Columb stress criterion is a theory which enables the analysis of rock mass made of rocks where UCS exceeds ultimate tensile strength (Steffen, 2017).

# 3. Numerical model

The numerical modelling steps include:
1. Construction of the model geometry (analyzed half of the model),
2. Development of the numerical grid,
3. Assigning mechanical properties,
4. Applying the boundary condition,
5. Initial numerical calculations.

## 3.1. Geometry

Numerical calculations were performed in order to determine the influence of changes in the compressive strength ($R_c$) of the roof strata and coal seam on the behaviour of the longwall in the mining system with a length of 30 m and height of 19 m (Fig. 2-a). The solid body of rock mass reflects the real working of a longwall located at a depth of 600 m. The discretization area of the examined rock mass, which represents the geometric domain, is shown in Fig. 2-b.
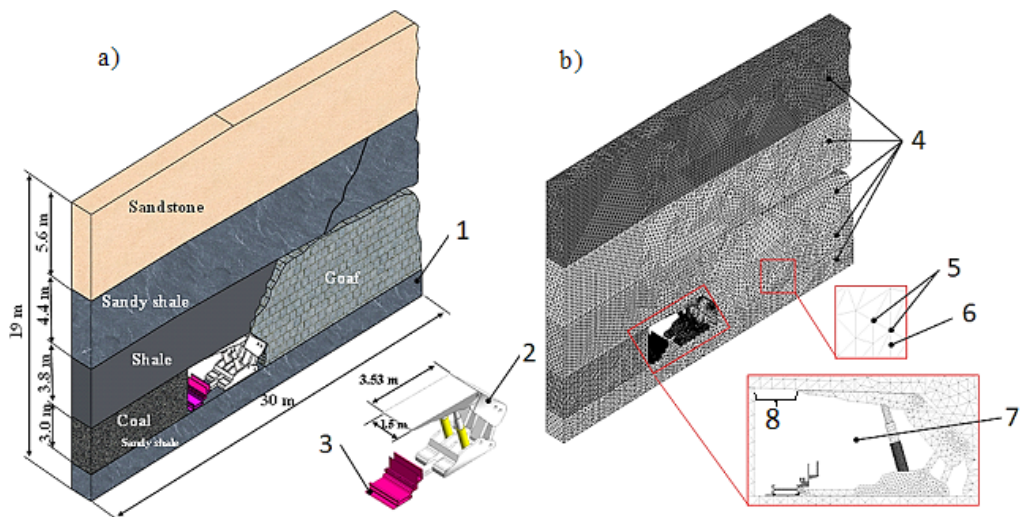


Fig. 2. Model geometry (a) and numerical grid (b) of rock mass with the 2-leg shield: 1 – rock mass, 2 – 2-leg shield, 3 – armored face conveyor (AMF), 4 – rock mass layers, 5 – nodes, 6 – elements, 7 – excavation (longwall working), 8 – tip-to-face distance

The powered roof support was installed in the longwall working. The longwall working was reflected as an excavation boundary. The length and height of the longwall working is 6.0 m and 3.0 m as shown in Fig. 2-a.The immediate roof is a shale stratum with a thickness of 3.8 m. Above the immediate roof is a sandy shale stratum with a thickness of 4.4 m. The floor is a sandy shale stratum with a thickness of 2.2 m.

## 3.2. Numerical grid

Figure 2-b illustrates the numerical grid of the analysed rock mass. The numerical grid was sliced into many small, simply shaped cells connected to each other at points called nodes. The numerical grid of the analysed longwall panel consisted of 7 blocks (Fig. 2-4) and 1 excavation boundary (Fig. 2-7). The excavation boundary simulates a longwall working, where a 2-leg shield was located. The numerical grid was defined by 312404 elements (Fig. 2-6) connected by 481466 nodes (Fig. 2-5).

## 3.3. Initial conditions

Six numerical models of rock mass were developed and analyzed in the model tests. They assessed the influence of the roof strata and coal seam mechanical properties and the 2-leg shield loading, as well as the interaction of the roof and floor on the stability of the longwall working, defined by the safety factor (FOS). The mechanical properties of the rock mass for different lithologies are shown in Table 3.

TABLE 3

Mechanical parameters of the rock mass lithologiesadopted in the calculations

| Rock | $\rho$ kg/m³ | $v$ – | $E$ GPa | $K$ GPa | $G$ GPa | $R_c$ MPa | $\varphi$ deg | $c_M$ MPa |
|---|---|---|---|---|---|---|---|---|
| Sandstone | 2650 | 0.38 | 21.1 | 29.30 | 7.64 | 50 | 25.45 | 10.4 |
| Sandy shale | 2670 | 0.29 | 17.6 | 13.96 | 6.82 | 35 | 25.40 | 8.3 |
| Shale | 2690 | 0.25 | 11.2 | 4.4 | 7.5 | **20** | 25.20 | 7.2 |
|  |  | 0.25 | 14.2 | 9.5 | 5.7 | **40** |  | 11.4 |
|  |  | 0.25 | 17.3 | 11.5 | 6.9 | **60** |  | 17.2 |
| Coal seam | 1450 | 0.24 | 4.7 | 3 | 1.8 | **10** | 24.20 | 4.2 |
|  |  | 0.24 | 6.7 | 4.2 | 2.7 | **20** |  | 8.3 |
| Goaf | 1440 | 0.4 | 0.1 | 0.16 | 0.03 | — | 12.0 | — |

$\rho$ – density, $v$ – Poisson's ratio, $E$ – Young's modulus, $K$ – elastic bulk modulus (Helmholtz module), $G$ – shear modulus (Kirchhoff module), $R_c$ – uniaxial compression strength, $\varphi$ – internal angle of friction, $c_M$ – cohesion.

The following boundary conditions were formulated:
– lower edges:define elastic support by normal stiffness to the face with a value of $1e^{10}$ MPa,
– lateral edges: displacement condition (fixed geometry in the $xy$ direction),
– the symmetry conditions to the faces of symmetry were applied,
– hydrostatic state of stress based on Equation (2),
– the angle of the roof fall line is equal to 65° for a mean compressive strength of rock strata between 19.6 and 60 MPa (Das, 2000),
– gravity $g = 9.81$ ms$^{-2}$.

The primary pressure in the rock mass was adopted in the numerical model based on the equation expressed in the following form (Biliński, 1968):

$$q = \gamma \cdot G \cdot m_c \cdot \cos(alpha) \qquad (2)$$

where: $m_c$ is a factor with a value of 0.5 [-] (Biliński, 1968), $\gamma$ is the specific gravity of rocks [MN m$^{-3}$], $q$ is the primary pressure [Pa], $G$ is the average exploration depth [m], cos(*alpha*) is the coal seam inclination angle [deg.].

The goaf was modelled as a solid block with low strength parameters and the height about 6.8 m. The goaf material was described by the values which are given in Table 3. The numerical models include the excavation of the coal seam by taking into account the situation after the web cut with value of a 0.80 m, including a longwall shearer with a length of 0.50 m. It means, that the tip-to-face distance is 1.30 m (Fig. 2-b).

## 3.4. Modelling of a 2-leg shield

The loading characteristics of the shield simulated in the numerical models are given in Figure 3. The 2-leg shield was analysed and it was located in the working of a longwall, operating at a seam height of 3.0 m and depth of 600 m. The geometrical construction of the 2-leg shield is a canopy (Fig. 3-1) with a length of 3.530 m, connected with hydraulic legs (Fig. 3-3)
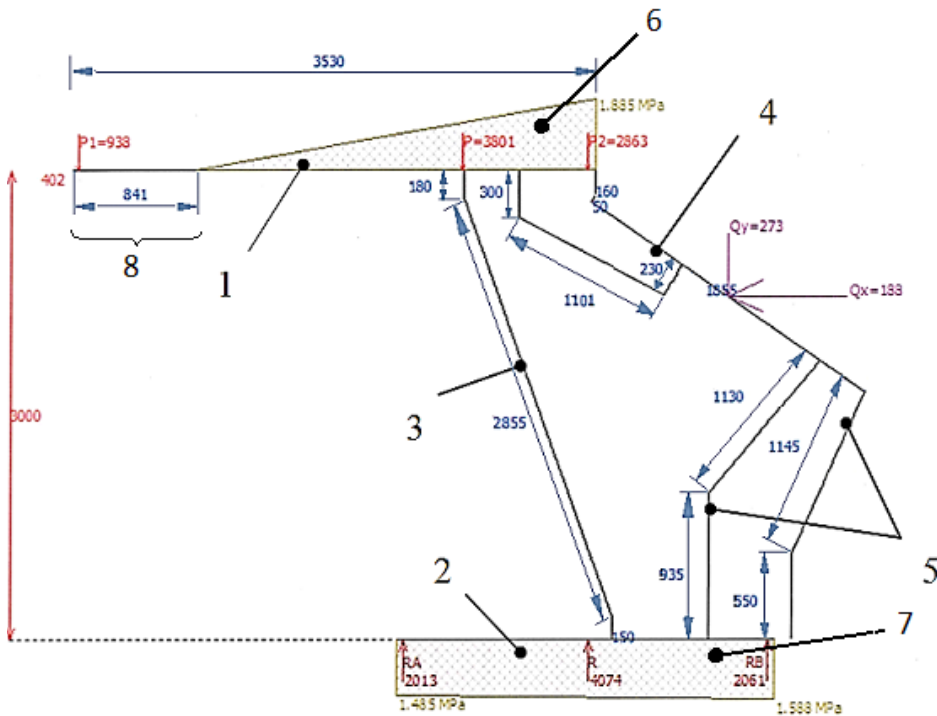


Fig. 3. Pressure distribution and geometry of the 2-leg shield: 1 – canopy, 2 – base, 3 – hydraulic legs, 4 – caving shield, 5 – lemniscate link, 6 – canopy load (stress concentration at canopy), 7 – base load (stress concentration at base), 8 – unsupported distance on the canopy, $P$ – vertical resultant force, $P1$ and $P2$ – components of the vertical resultant force [kN], $R$ – vertical reaction force [kN], $RA$ and $RB$ – components of the vertical reaction force [kN], $Qy$ – caving shield vertical component force [kN], $Qx$ – caving shield horizontal component force [kN]

with a diameter of 280 mm and a length of approximately 2.855 m, and a base (Fig. 3-2) with a length of approximately 2.650 m. The canopy and the base are connected with a caving shield at approximately 2.260 m (Fig. 3-4) and linked with lemniscate at approximately 1.130 m and 1.145 m (Fig. 3-5). Simulations were performed for 2-leg shield which was characterized by the technical parameters as follows:

- coefficient of friction between the rock mass and 2-leg shield: $\mu = 0.3$,
- shield height range: 1.6 to 3.2 m,
- section pitch: 1.5 m,
- leg diameter: 0.280 m,
- support advancing force for 25 to 32 MPa: 1.54 to 1.97 MN,
- operational pressure in the legs: 38 MPa (2.28 MN).

The pressure distribution along the canopy of the 2-leg shield shows a trapezoidal distributed loading characteristic with a maximum value of 1.885 MPa. Similar to the canopy, the pressure distribution along the base shows a trapezoidal distributed loading characteristic with minimum and maximum values of 1.485 MPa and 1.558 MPa, respectively.

# 4. Results

## 4.1. Roof capacity index 'g'

Based on the 2-leg shield capacity ($M_P$) and the load of the support ($M_Q$) as well as the mechanical parameters listed in Table 3, the roof capacity index 'g' was calculated in order to determine the influence of changes in the compressive strength ($R_c$) of the roof strata and coal seam on the stability of the longwall. The value of index 'g' for the analyzed longwall is presented in graphic form in Figure 4 and Figure 5. The vertical axis describes the roof capacity. The horizontal axis describes the mining velocity.

The correct use of different types of powered supports in a longwall, following the principle of the appropriate values of the roof capacity index 'g', can be determined as follows:

- if in the same height range and the same roof and floor conditions, all shields enable a roof capacity index 'g' of the floor layers, characterizing the maintenance condition of the longwall working roof, of equal to or greater than 0.8 to be obtained, then their simultaneous use is recommended and their selection is optimal,
- if, in the same height range and under the same roof and floor conditions, one shield enables a roof capacity index 'g' of the floor strata equal to or greater than 0.8 to be obtained, and another shield provides a index 'g' of the floor strata equal to or greater than 0.7, but less than 0.8 it is possible to use them simultaneously, but their selection is not optimal,
- if, in the same height range and the same roof and floor conditions, the shield enables a roof capacity index 'g' of the floor strata equal to or greater than 0.7 but less than 0.8 to be obtained, their simultaneous use is possible but not optimal,
- if in the same height range and the same roof and floor conditions, one of the shields does not enablea roof capacity index 'g' of the floor strata greater than or equal to at least 0.7 ('g' is less than 0.7) to be obtained, simultaneous use (from the point of view of cooperation between the shield and the rock mass) is not recommended.
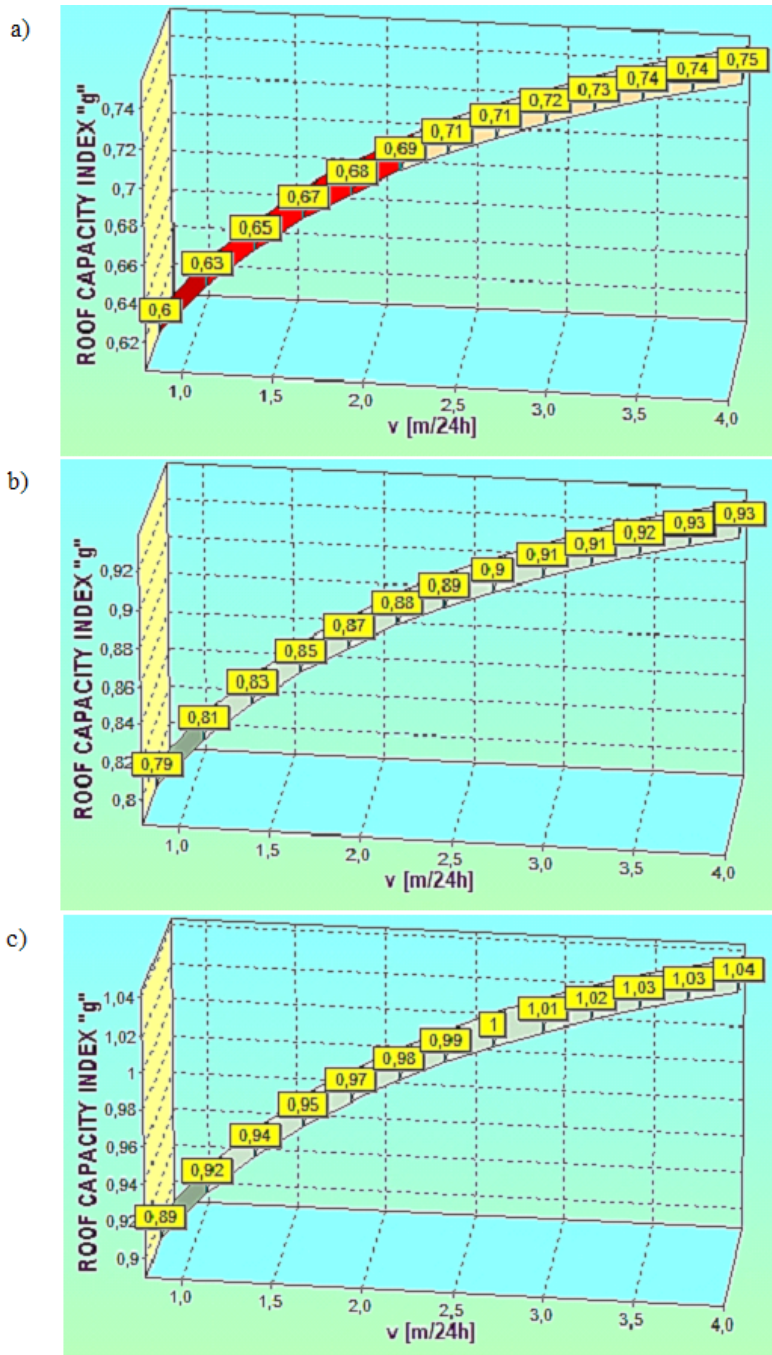
Fig. 4. Analysis of roof capacity index 'g'for coal seam compressive strength of 10 MPa:
a – for roof compressive strength of 20 MPa, b – for roof compressive strength of 40 MPa,
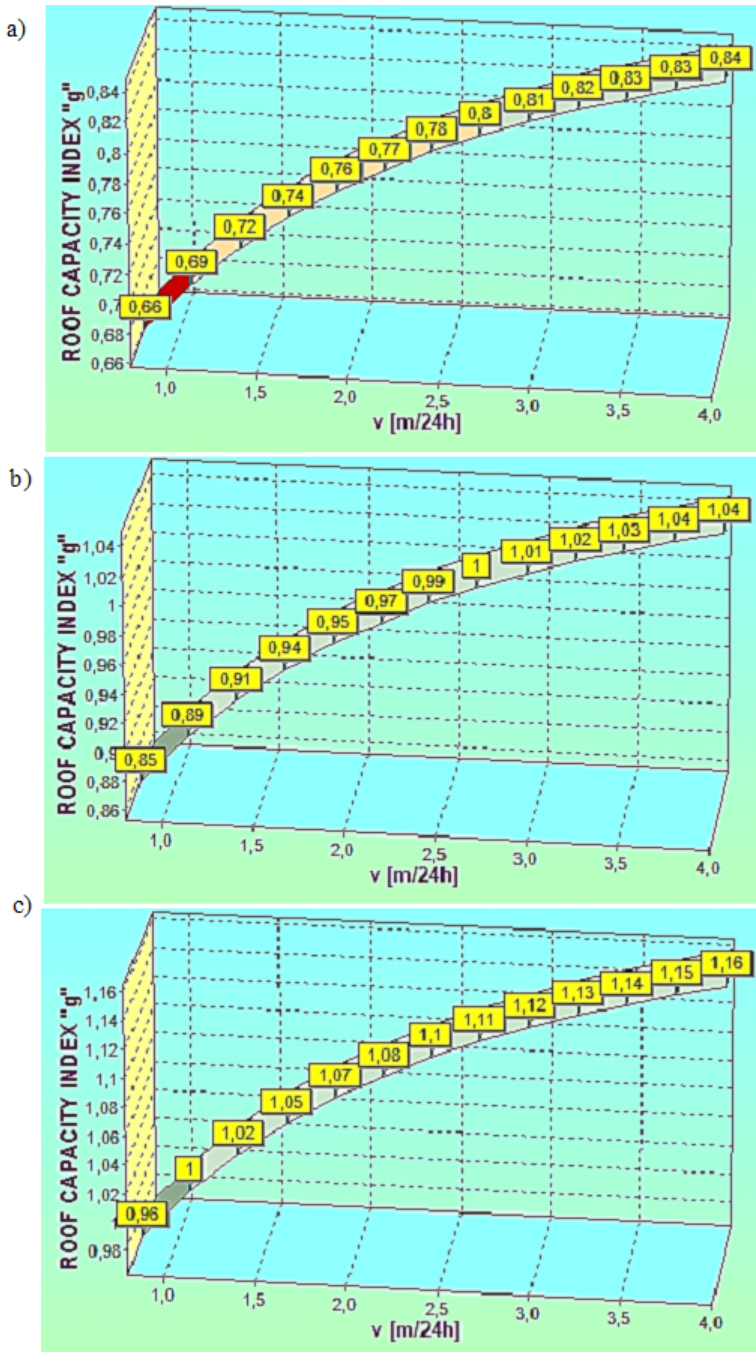c – for roof compressive strength of 60 MPa

502



Fig. 5. Analysis of roof capacity index 'g' for coal seam compressive strength of 20 MPa:
a – for roof compressive strength of 20 MPa, b – for roof compressive strength of 40 MPa,
c – for roof compressive strength of 60 MPa

To summarize, when using the roof capacity index 'g' for the assessment of the conditions for roof maintenance in a longwall panel, the following criteria should be adopted:

– $g < 0.7$ – very bad roof maintenance,
– $0.7 \leq g < 0.8$ – difficult conditions for roof maintenance,
– $g \geq 0.8$ – good or very good roof maintenance.

The obtained values of the roof capacity index 'g' indicate that there may be very poor (Fig. 4a and Fig. 5a) and difficulties conditions for roof maintenance (Fig. 4b and Fig. 5b). Good or very good conditions for roof maintenance occur for compressive strength of 60 MPa (Fig. 4c and Fig. 5c). The obtained values of the roof capacity index 'g' lead to the conclusion that it will be beneficial to lead the longwall with the greatest mining advancing due to the fact that an increase in mining advancing, generally increases the value of roof capacity index 'g'.

## 4.2. Factor of safety (FOS)

The value of FOS index was simulated in order to assess the safety of the region in the rock mass model with interaction with a 2-leg shield (Fig. 3). For this purpose, the values of the compressive strength ($R_c$) of the roof strata and coal seam were taken into account and are listed in Table 3. The 2-leg shield setting pressure was selected as 25 MPa. SolidWorks software enables the determination and the ability to view the plot of FOS distribution throughout the entire solid body model. The critical regions of the analyzed rock mass were plotted in Figure 6÷11 in the form of a map, where ultimate strength is exceeded and the safety factor is less than 1. The
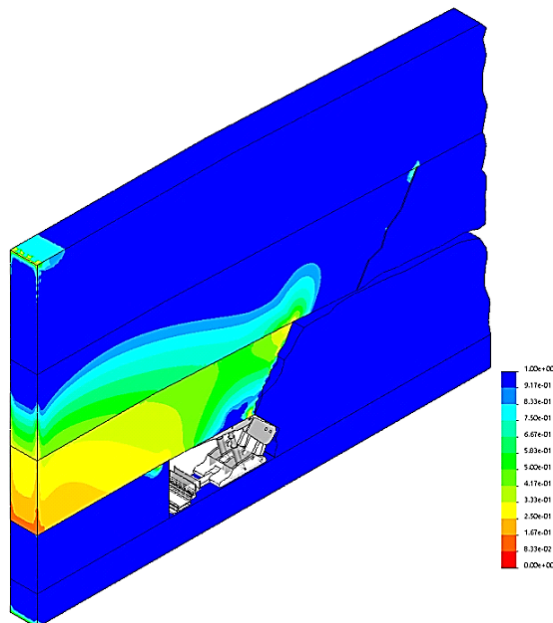


Fig. 6. Analysis of FOS index for coal seam compressive strength of 10 MPa under the roof compressive strength conditions of 20 MPa

504

analysis of results was conducted on a part of unsupported roof between the tip of canopy and the coal face, at the distance of 1.3 m (Fig. 2b).

The results in Figure 6 shows, that in the case the compressive strength of the roof is 20 MPa and the coal seam compressive strength is 10 MPa, the value of the FOS index varies from 0.25 to 0.51.
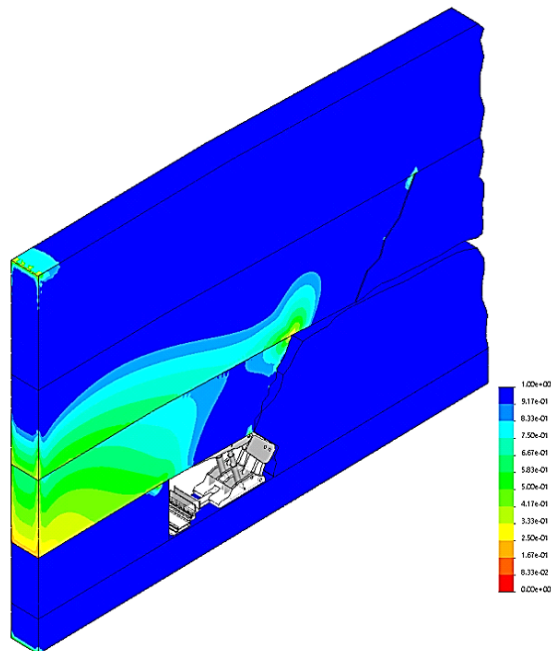
The results in Figure 7 shows, that in the case the compressive strength of the roof is 40 MPa and the coal seam compressive strength is 10 MPa, the value of the FOS index varies from 0.50 to 0.58.



Fig. 7. Analysis of FOS index for coal seam compressive strength of 10 MPa under the roof compressive strength conditions of 40 MPa

The results in Figure 8 shows, that in the case the compressive strength of the roof is 60 MPa and the coal seam compressive strength is 10 MPa, the value of the FOS index varies from 0.76 to 1.0.

The results in Figure 9 shows, that in the case the compressive strength of the roof is 20 MPa and the coal seam compressive strength is 20 MPa, the value of the FOS index varies from 0.35 to 0.57.

The results in Figure 10 shows, that in the case the compressive strength of the roof is 40 MPa and the coal seam compressive strength is 20 MPa, the value of the FOS index varies from 0.57 to 0.85.

The results in Figure 10 shows, that in the case the compressive strength of the roof is 40 MPa and the coal seam compressive strength is 20 MPa, the value of the FOS index varies from 0.82 to 1.0.
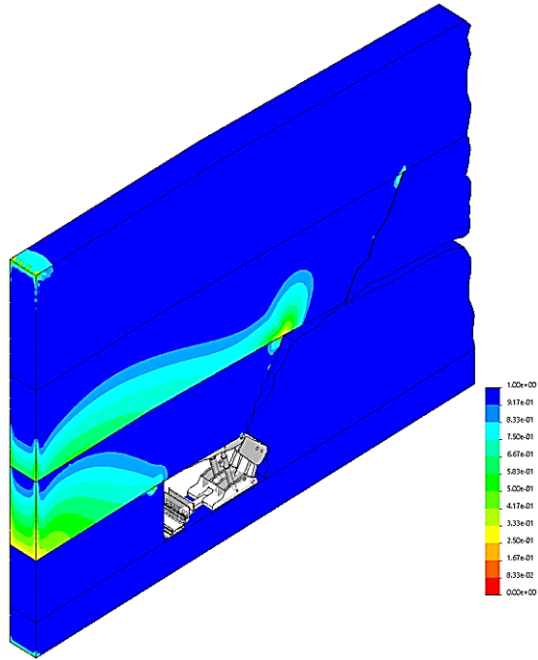
Fig. 8. Analysis of FOS index for coal seam compressive strength of 10 MPa under the roof compressive
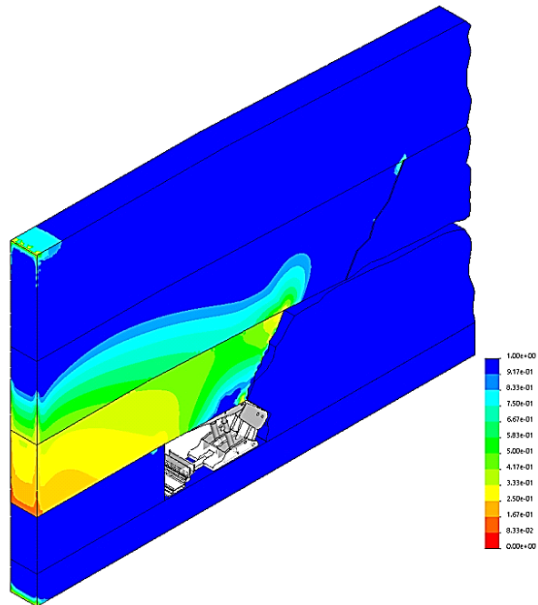strength conditions of 60 MPa



Fig. 9. Analysis of FOS index for coal seam compressive strength of 20 MPa under the roof compressive
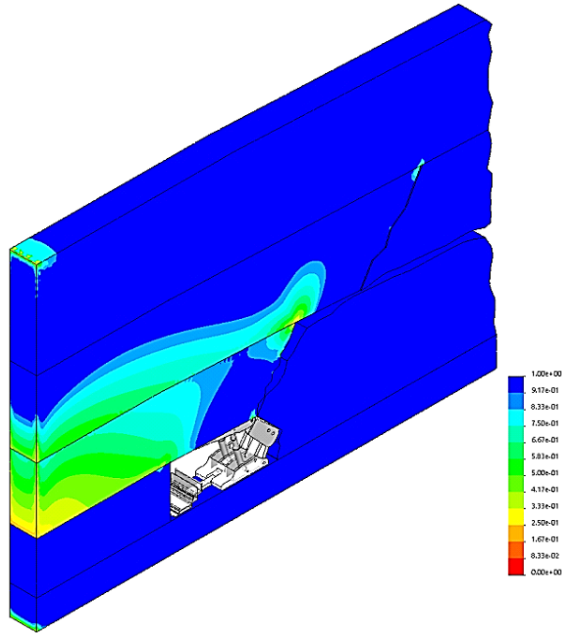strength conditions of 20 MPa

506



Fig. 10. Analysis of FOS index for coal seam compressive strength of 20 MPa under the roof compressive strength conditions of 40 MPa
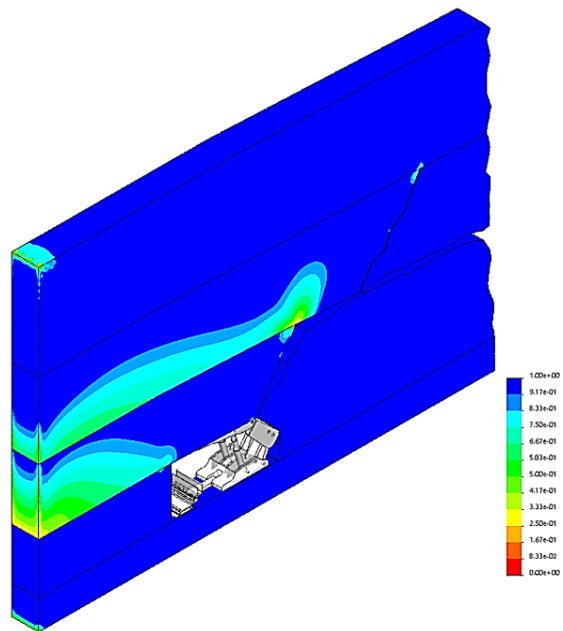


Fig. 11. Analysis of FOS index for coal seam compressive strength of 20 MPa under the roof compressive strength conditions of 60 MPa

It can be concluded, that the unsafe regions are shown in Figures 6÷7 and Figures 9÷10, where the factor of safety is less than 1.0. The safe regions are shown in Figure 8 and Figure 11, where the safety factor is greater than 1.0.

## 4.3. Result analysis

The analysis of results was performedin order to estimate the existence of the correlation coefficient between tested indexes as well as to demonstrate the impact of the roof capacity index 'g' value on the factor of safety (FOS). In Table 4 values of roof capacity index 'g' and FOS (average) depending on the UCS of roof and coal in longwall working are shown.

TABLE 4

Roof capacity index 'g' and the factor of safety (FOS) depending on theuniaxial compression strength (UCS) of the coal and roof in a longwall

| UCS ($R_c$) of coal, [MPa] | UCS ($R_c$) of roof, [MPa] | Roof capacity index 'g', [-] | FOS, [-] |
|---|---|---|---|
| 10 | 20 | 0.6 | 0.38 |
|  | 40 | 0.79 | 0.54 |
|  | 60 | 0.89 | 0.88 |
| 20 | 20 | 0.66 | 0.46 |
|  | 40 | 0.85 | 0.71 |
|  | 60 | 0.96 | 0.91 |

The effects of the analysis are shown in Figure 9 and Figure 10. In the case where the UCS of coal is 10 MPa and the UCS of roof is changing in the range from 20 MPa to 60 MPa, the value of the correlation is 0.86 (Fig. 12). It means that a strong relationship exists between the analyzed values.
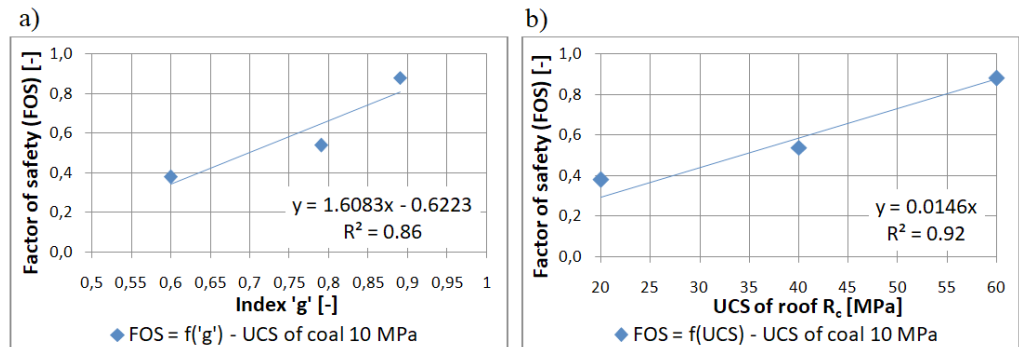
a)    b)



Fig. 12. The change in the factor of safety (FOS) depending on the roof capacity index 'g' (a) and the UCS of roof (b) for coal seam compressive strength of 10 MPa

In the case where the UCS of coal is 20 MPa and the UCS of the roof is changing in the range from 20 MPa to 60 MPa, the value of the correlation coefficient is 0.99 (Fig. 13). It means that a very strong relationship exists between the analyzed values.
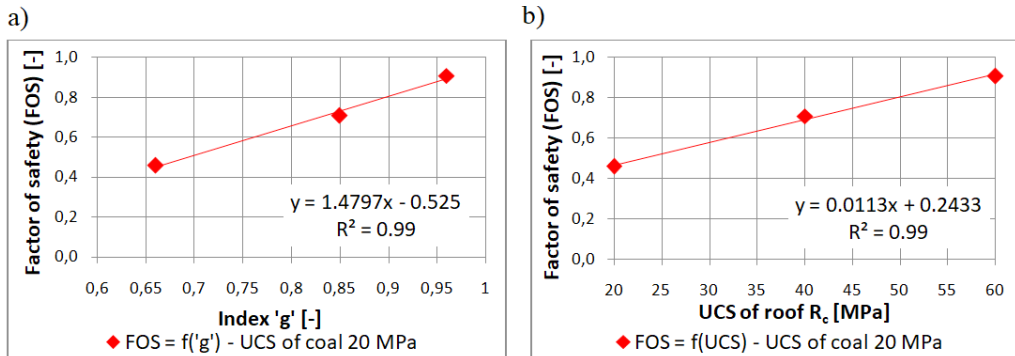
a)

b)

Fig. 13. The change in the factor of safety (FOS) depending on roof capacity index 'g'(a)
and the UCS of roof (b) for coal seam compressive strength of 20 MPa

# 5. Conclusions

This research work consists of the modelling of a longwall panel in order to investigate the stability of a roof in the working of a longwall. The stability of the longwall panel was estimated by determining the factor of safety (FOS). This method, based on the Mohr-Columb stress criteria, enables the prediction of the occurrence of roof failure when both the maximum tensile principal stress $\sigma_1$ and the minimum compressive principal stress $\sigma_3$ exceed their respective stress limits.

Based on the results of numerical modelling, the following conclusions were reached:

- demonstrating the linear relationship between the roof capacity index 'g' and safety factor (FOS) shows that the FOS method enables the description and prediction of the conditions for roof maintenance in a longwall,
- the numerical analysis proved that the factor of safety (FOS) provides an alternative method for analyzing roof stability in the working of a longwall,
- the factor of safety (FOS) provides an alternative method for selecting a shield for given mining conditions.
- presented method may be utilized in evaluating the mining natural hazards through predicting the main parameters which determine the roof maintenance in the longwall working.

### Acknowledgment

### References

Biliński A., 1968. *The symptoms of rock mass pressure in longwall panels located in hard coal seam.* Zeszyt Naukowy nr 221, Górnictwo z. 31, Politechnika Śląska, Gliwice, [In Polish]

Das S.K., 2000. *Observations and classification of roof strata behaviour over longwall coal mining panels in India*. International Journal of Rock Mechanics and Mining Sciences **37**, 585-597.

Düzgün H.S.B., 2005. *Analysis of roof fall hazards and risk assessment for Zonguldak coal basin underground mines*. International Journal of Coal Geology **64**, 1-2, 104-115.

Duzgun H.S.B., Einstein H.H., 2004. *Assessment and management of roof fall risks in underground coal mines*. Safety Science **42** (1), 23-41.

Ghasemi E., Ataei M., Shahriar K., Sereshki F., Jalali S.E., Ramazanzadeh A., 2012. *Assessment of roof fall risk during retreat mining in room and pillar coal mines*. International Journal of Rock Mechnics and Mining Sciences **54**, 80-89.

Ghasemi E., Ataei M., Shahriar K., 2017. *Improving the method of roof fall susceptibility assessment based on fuzzy approach*. Archives of Mining Sciences **1**, 13-32.

Gu S., Jiang B., Wang G., Dai H., Zhang M., 2018. *Occurrence mechanism of roof-fall accidents in large-section coal seam roadways and related support design for bayangaole coal mine, China*. Advances in Civil Engineering 2018, Article ID 6831731, 17.

Iannacchione A., Bajpayee T.S., Prosser L., 2007. *Methods for determining roof fall risk in underground mines*. Min. Eng. **59** (11), 47-53.

Labuz J.F., Zan A., 2012. *Mohr-Coulomb Failure Criterion.* Rock Mech. Rock Eng. **45**, 975-979

Mark C., Pappas D.M., Barczak T.M., 2011. *Current trends in reducing groundfall accidents in U.S. coal mines*. Min. Eng. **63** (1), 60-66.

Martyka J., Hetmańczyk P., 2013. *Annual report: The state of natural and technical hazards in Polish hard coal mines in 2013*. Report under Prof. Kabieszlidership, GIG, Katowice, 15-27 [In Polish].

Palei S.K., Das S.K., 2008. *Sensitivity analysis of support safety factor for predicting the effects of contributing parameters on roof falls in underground coal mines*. Int. J. Coal Geol. **75**, 241-247.

Petrova R.V., 2015. *Introduction to Static Analysis Using SolidWorks Simulation*. CRC Press, London.

Prusek S., Rajwa S., Wrana A., Krzemień A., 2017. *Assessment of roof fall risk in longwall coal mines*. International Journal of Mining, Reclamation and Environment **31** (8), 558-574.

Rajwa S., Janoszek T., Prusek S., 2020. *Model tests of the effect of active roof support on the working stability of a longwall*. Computers and Geotechnics 118, 103302. https://doi.org/10.1016/j.compgeo.2019.103302

Rajwa S., Janoszek T., Prusek S., 2019. *Influence of canopy ratio of powered roof support on longwall working stability – A case study*. International Journal of Mining Science and Technology **29** (4), 591-598.

Steffen J., 2018. *Analysis of Machine Elements Using SolidWorks Simulation 2012*. SDC Publications.

Walentek A., Lubosik Z., Prusek S., Masny W., 2009. *Numerical Modelling of the Range of Rock Fracture Zone around Gateroads on the Basis of Underground Measurement Results*. 28th International Conference on Ground Control in Mining. USA, Morgantown s. 121÷128.